MITSUBISHI ELECTRIC RESEARCH LABORATORIES
http://www.merl.com

A Numerical Study of Refrigerant Dispersion in Single and Multiple Connected Spaces

Laughman, C.R.; Nabi, S.; Grover, P.

TR2016-018 January 2016

Abstract

While the possible impact of refrigerant leaks and subsequent dispersion in an occupied space pertains to a wide variety of applications, dynamic models that accurately describe dispersion phenomena in the built environment have not been extensively explored in the literature. This paper builds on work published in (Laughman, Nabi and Grover 2015) by assessing the performance of well-mixed models via a comparison to computational fluid dynamics simulations and studying the behavior of refrigerant dispersion in multiple connected spaces. Results indicate that the well-mixed models are not able to capture variation in the geometric parameters very accurately, and should be used cautiously, while the studies of the dynamics in multiple spaces highlights the importance of the location of ventilation sources and sinks.

2016 ASHRAE Winter Meeting

A Numerical Study of Refrigerant Dispersion in Single and Multiple Connected Spaces

ABSTRACT

While the possible impact of refrigerant leaks and subsequent dispersion in an occupied space pertains to a wide variety of applications, dynamic models that accurately describe dispersion phenomena in the built environment have not been extensively explored in the literature. This paper builds on work published in (Laughman, Nabi and Grover 2015) by assessing the performance of well-mixed models via a comparison to computational fluid dynamics simulations and studying the behavior of refrigerant dispersion in multiple connected spaces. Results indicate that the well-mixed models are not able to capture variation in the geometric parameters very accurately, and should be used cautiously, while the studies of the dynamics in multiple spaces highlights the importance of the location of ventilation sources and sinks.

INTRODUCTION

Efforts to understand the behavior of refrigerant dispersion and mitigate its consequences have accompanied the development of vapor compression cycles since very early in the development of this technology. Such efforts in the U.S. by members of ASRE led to the development of a safety code, first published 100 years ago, that was intended to prescribe and codify practices that would assure the safety of building occupants and refrigeration engineers in the face of the risks of refrigerant exposure (Reindl 2014). The original document has been adapted and modified periodically over the intervening years to cover the wide range of new equipment and applications that have emerged, and its scope is now covered by ASHRAE Standard 34 (Designation and Safety Classification of Refrigerants) (ASHRAE Standard 34 2010), which assigns safety classifications for refrigerants based upon toxicological and flammability data, and ASHRAE Standard 15 (Safety Standard for Refrigeration Systems) (ASHRAE Standard 15 2010), which pertains to the construction of systems that incorporate refrigerant pipes that pass through occupied spaces. Standard 15 provides guidance that affects many aspects of air-conditioning and refrigeration systems, such as the specification of pressure relief valves and pressure vessels, as well as limitations on the amount of refrigerant allowed in systems with pipes passing through occupied spaces to minimize the impact of potential refrigerant leaks on occupant safety.

Because Standard 15 is designed to be applied as a prescriptive standard by local code enforcement authorities, it uses an extremely simple model to describe the behavior of refrigerant leakage phenomena. This model is based upon the refrigerant concentration limit (RCL) identified by Standard 34, and is essentially an algebraic calculation of the maximum mass of refrigerant that may be charged into a system that has pipes in the space under consideration. The standard does not incorporate a dynamic model describing the time-dependent behavior of the leaks, nor does it describe the dynamics of the refrigerant dispersion; instead, it effectively assumes that all of the refrigerant in the system appears in the occupied space instantaneously. A given system installation is threfore permitted by the standard if the evacuation of its complete charge into a space would not exceed the RCL, and is prohibited otherwise.

While this method of characterizing the effects of refrigerant leaks is appealing because of its simplicity, the resulting system design criteria are extremely conservative and can significantly constrain the system specification. For buildings that comply with other ASHRAE standards, such as (ASHRAE Standard 62.1 2013), the concentration in the room will not approach the RCL for a variety of leakage rates because of ventilation; thus, there are scenarios in which a system deemed unacceptable under Standard 15 will actually present no safety hazard (Waye, Petersen and Beyer-Lout 2012). Questions can therefore arise about the suitability of Standard 15 for some types of equipment, such as VRF systems, because of these stringent standards (Duda 2012). Such a general methodology, coupled with the absence of a quantitative risk analysis-based approach, can result in limitations on system specification that can have a significant economic effect on building owners and occupants without improving occupant safety because of prohibitions on the installation of more effective or energy-efficient space-conditioning systems than are permitted under current practice.

One organization that has been collecting and assessing the impact of refrigerant leaks on building occupants for some time is the High Pressure Gas Safety Institute of Japan (Kouatsu-Gas Hoan Kyoukai, or KHK). Since its founding in 1963, this group has collected data on refrigerant leakage incidents, and can provide valuable historical information which, when coupled with information about Japanese refrigerant safety standards, can provide quantitative data about the efficacy of safety measures. This organization collects a wide range of information on refrigerant leaks; any incident that requires emergency services is reported, as well as any significant release (a leak greater than would result in the gradual formation of very small bubbles with leak-checking fluid) by authorized facilities (O. Kataoka 2015). In their annual report for 2013, for example, KHK recorded 118 refrigerant leakage incidents in all of Japan, of which 52 could be ascribed to leaks in pipes, 40 due to leaks in heat exchangers, and 23 due to leaks in valves. Of the larger refrigerant leaks that are described in detail, most are low-rate leaks that occurred due to corrosion, pinholes, or small cracks created when water around the pipes froze. These events predominantly were noted after they occurred by service technicians, and were not reported by building occupants (KHK 2014). Given the predominance of split-ductless and VRF systems in Japan, it is interesting to note the very low incidence of significant leaks affecting occupant safety.

There are also ambiguities in Standard 15 that can raise questions during its application, either in regard to its scientific foundation or to vagueness in its language because the standard does not provide any technical publications relating to refrigerant dispersion in its informative references and because this simplified analysis is directly applied to the complex built environment. For example, one ambiguity in this standard relates to the determination of whether two adjacent occupied spaces are connected by a permanent opening, though the phrase ``permanent opening'' is not defined. In describing the calculation of the room volume for the purposes of determining the maximum system charge, Section 7.3 uses this definition to state that the volume of the smallest occupied space to which a refrigerant leak would disperse shall be used to determine the refrigerant concentration limit in the refrigerating system when the parts of that system are located in one or more enclosed occupied spaces that do not connect through such permanent openings or HVAC ducts. While this section addresses the practical reality that two rooms may be joined by a small connecting volume, such as a door undercut or a small transfer opening, it does not provide the reader with the information needed to determine whether a given opening is sufficient to use the combined volume of both rooms in the determination of the maximum allowable refrigerant mass for a given system.

(Laughman, Nabi and Grover 2015) suggests one strategy for addressing these limitations that would lead to the development of new models and the use of modern quantative risk assessment methodologies to evaluate more realistic bounding scenarios for assuring occupant safety while maintaining the current methodology's ease of use. This strategy involves the partitioning the overall problem into two related subproblems: one pertaining to the determination of the potential leakage rates due to the refrigerant system and cycle architecture, and another involving the dynamics of the dispersing refrigerant into the occupied space. Improved models of the refrigerant leak dynamics would facilitate the use of time- or exposure-based methods for predicting occupant safety, which would be inherently more realistic and would more easily extensible to future innovations in system architectures, since the leakage rates are dependent on the cycle architecture. Moreover, such models would enable the assessment of more realistic leakage scenarios, thereby reducing the number of constraints on system specification while maintaining acceptable safety thresholds.

The importance of understanding and characterizing the dynamics of refrigerant dispersion, which is particularly pertinent to the ongoing transition to fourth-generation flammable refrigerants, has elicited a variety of recent work in understanding the dynamics of refrigerant dispersion in occupied spaces. (Waye, Petersen and Beyer-Lout 2012) studied the problem of refrigerant dispersion specifically for the case of ventilating mechanical rooms, and discussed both the shortcomings of the current method and possible alternative models which described the dispersion dynamics more accurately. In relation to the distribution of flammable refrigerants, (Kataoka, Ishida, et al. 1999) studied different refrigerant releases in both simulation and experiment, and explored a range of important parametric variation, including the refrigerant leakage rate, the concentration gradients in the occupied space, the leak height, and the effect of mechanical circulation. Other recent publications by (Nagaosa, Aute and Radermacher 2012), (Lewandowski and Reid 2012), and (Okamoto, et al. 2014) also study the dynamics of refrigerant dispersion; however, the exclusive focus of the work discussed is the possibility of combustion for a variety of relevant working fluids, such as ammonia, R600a, R1234yf, and R32, rather than studying the transient behavior of the refrigerant concentration in the space. Similar work has also been performed by JSRAE, and is discussed in detail in (Hihara 2014).

This work explores two main topics relating to the functionality and development of new models for refrigerant dispersion dynamics. The first of these examines the applicability of the well-mixed assumption to refrigerant dispersion events. (Waye, Petersen and Beyer-Lout 2012) proposed such well-mixed models for use in describing refrigerant dispersion dynamics because these models are simple and can characterize the time-varying dynamics of the refrigerant concentration in the room. However, the work of (Laughman, Nabi and Grover 2015), which used computational fluid dynamics (CFD) tools to simulate the dynamics of refrigerant dispersion, indicated that the distribution of refrigerant under some ranges of parameters was very stratified. Consequently, one main focus of the present work is the evaluation of the assumptions inherent to the well-mixed models, as well as accuracy of these models' performance under a variety of circumstances.

The second objective of this paper is the study of the effects of parametric variation on the refrigerant distribution in two connected rooms. There are few extant publications related to this topic, which is of central importance to a code-enforcement authority who is evaluating the safety of a particular system in the field. This work was therefore designed to address the ambiguity about connecting spaces that is in the present version of Standard 15, and develop a baseline set of information about the dynamics of how refrigerant is distributed in multiple connected rooms as a function of the refrigerant leakage rate, the relative room size, and the exhaust air flow rate.

The remainder of this paper is structured to address both of these objectives in separate sections, and highlight promising directions for future work. Section 2 briefly describes the background of the underlying equations describing the fluid flow, as well as the construction of the CFD simulations that were used to describe the refrigerant dispersion dynamics. Section 3 then develops a set of well-mixed models, and studies the ability of these models to represent the dynamics observed in the CFD simulations. Section 4 extends these analyses to the two-room scenarios, and discusses both the effects of parametric variation on the distribution of refrigerant in each of the connected rooms as well as how the current version of Standard 15 might be applied to such multiple connected spaces. Finally, conclusions and directions for future work will be presented in Section 5.

SIMULATION BACKGROUND

This simulation study of the efficacy of well-mixed models and the dynamics of refrigerant dispersion in multiple connected spaces was carried out on single room and two room test cases, respectively. The single room geometry comprised a cubic space that was 3.04 m (10 ft) on a side, while the two room simulations included one space with the above dimensions as well as a second space of the same height and length as the first, but with half of the width. These room geometries are illustrated in Figure 1; the single room simulations used to evaluate the well-mixed models are referred to the ``forced" room which contains the refrigerant injection source only, while the two room simulations also include the adjacent ``unforced" room. These candidate geometries, which resemble the dimensions of small hotel rooms or offices, were selected because they represent small occupied spaces and could serve as useful bounding cases to examine the dynamics of refrigerant dispersion, since the observed effects would not be as consequential in larger spaces. The refrigerant R410A, which has an RCL of 420 g/m^3 (0.026 lb/ft^3) (ASHRAE Standard 34 2010), was used for all of these simulations.

As the work presented in this paper is focused on two different explorations, the range of parametric variation differs between the single room and the two room scenarios. Because the single room simulations examined the manner by which the effects of parametric variation were manifest in the degree of stratification, the set of parameters chosen for variation included the mass flow rate of refrigerant $\dot{m}_{ref}$, the exhaust air flow rate Q_{exh}, the height of the door undercut h_{out}, and the location of the refrigerant injection. Two different mass flow rates of refrigerant were use to characterize the leaks, as there is currently no consensus regarding appropriate refrigerant leakage rates for such studies: the value specified in Appendix E of (UL 484 2012), 25% of the system charge in 1 minute, or 75 g/s (9.9 lb/min) was used to characterize the effect of high leak rates, also referred to as $\dot{m}_{high}$, while the value specified in (ISO 5149-3 2014) of 2.5 g/s (0.325 lb/min) was used to characterize the effect of low leak rates, also referred to as $\dot{m}_{low}$.

In comparison, the two-room simulations were designed to study the variation in the refrigerant dispersion dynamics due to parameters specifically associated with multiple connected rooms. This list of parameters includes the height h_{in} and width w_{in} of the undercut connecting the two rooms, the choice of room in which the exhaust vent was located, the relative size of the two rooms, and the location of the refrigerant injection. The effect of varying the refrigerant leak rate was also studied in these simulations. A full search of such a range of parameters was not feasible due to the sheer amount of computational time required to explore such a large space, but a series of salient observations are collected in this paper that proved to illuminate important dynamics of the refrigerant dispersion phenomena.

CFD simulations were used to study the temporal and spatial behavior of the refrigerant leaks in these enclosed spaces due to the nonlinear and spatially-distributed nature of the refrigerant flow. The following governing partial differential equations describe the mean flow properties for the three-dimensional time-dependent flow (Bird, Steward and Lightfoot 2006), (White 2005):

Mixture mass (continuity)
$$\frac{\partial \rho}{\partial t} + \nabla \cdot (\rho \mathbf{V}) = 0$$

Mixture momentum (Navier-Stokes)
$$\frac{D\rho\mathbf{V}}{Dt} = -\nabla P + \nabla \cdot \left(\mu_{eff}(\nabla\mathbf{V} + \nabla\mathbf{V}^{\mathrm{T}})\right) + \rho\mathbf{g}$$

Mixture enthalpy
$$\frac{D\rho H}{Dt} = \nabla\left(\frac{\mu_{eff}}{\sigma}\nabla H\right) + \frac{DP}{Dt}$$

Species transport (total mass fraction)
$$\frac{D\rho Y_i}{Dt} = \nabla\left(\frac{\mu_{eff}}{\sigma}\nabla Y\right)$$

where ρ is the mixture density, $\boldsymbol{V}$ is the vector of fluid velocities along the axes of the coordinate system, μ_{eff} is the effective mixture viscosity, H is the mixture specific enthalpy, $\boldsymbol{g}$ is the gravitational acceleration, σ is the mixture surface tension, P is the pressure, and Y_i is the mass fraction of the i^{th} component. The mixture density ρ is related to the component densities ρ_i and mass fractions Y_i by

$$\frac{1}{\rho} = \sum \frac{Y_i}{\rho_i} \tag{1}$$

$$\sum Y_i = 1 \tag{2}$$

and the material derivative is defined as

$$\frac{Dy}{Dt} = \frac{\partial y}{\partial t} + \mathbf{V} \cdot \nabla y \tag{3}$$

These governing equations, as well as the two equation $k - \omega$ turbulence closure model described in the cited literature, were solved with the commercial solver ANSYS CFD (CFX 15.0) (ANSYS CFX-Pre User's Guide, Release 15.0 2014) by implementing the finite volume method on a three-dimensional unstructured mesh. An ideal gas model of air was used, while a real gas model of the refrigerant R410A was used to describe the leaking fluid. A higher-order scheme was used to discretize the convective and diffusive terms, and a second-order backward Euler method was implemented for temporal discretization. A grid system with a sample density on the order of $N \sim \mathcal{O}(10^5)$ and an adaptive time-stepping method with the largest time steps on the order of $\Delta t \sim \mathcal{O}(10^{-1})$ were used to solve these models. Additional information on the model implementation in the CFD tools is provided in (Laughman, Nabi and Grover 2015).

SINGLE ROOM WELL-MIXED MODELS

The question of how to develop an accurate model with low computational requirements is a central task in developing a means for code-enforcement authorities to evaluate the safety of refrigerant pipes in occupied spaces without being constrained by the limitations of the static approach used in current standards. Such models would likely be used to evaluate the time-varying average refrigerant concentration in the space to assess whether it will exceed the RCL at any point in time and for how long. These models have many requirements, including the ability to accurately predict or construct bounds on the average refrigerant concentration in a space, the ability to be parametrized using common characteristics (e.g., exhaust or ventilation flow rates, door undercuts), and be executed in a reasonable amount of time. While contemporary CFD methods are able to describe the dynamics of refrigerant dispersion in a very detailed manner, they are generally too expensive, too complex, and take too long to run with current technology, and are therefore not generally appropriate for most applications.

Well-mixed models (Waye, Petersen and Beyer-Lout 2012) are a class of candidate models that can describe the dynamic behavior of the refrigerant concentration while maintaining relatively low computational requirements. These models are based upon the assumption that all of the refrigerant in a given space is uniformly distributed, and can describe the time evolution of this average concentration as more refrigerant is added to the space via a leak or is removed through air exchange with an external environment. By ignoring the spatial inhomogeneity in the room, this ``well-mixed" assumption makes it possible to describe the temporal evolution of the refrigerant concentration via an ordinary differential equation (ODE) that allows the refrigerant concentration to be solved analytically or numerically, rather than the more complex partial differential equations (PDEs) described in the Navier-Stokes equations. In comparison, the PDE models describe spatially-varying behavior in which the the refrigerant reaches the bottom of the building zone and spreads along the walls and form a more concentrated layer at floor at the start of the injection, due to both the initial momentum of the refrigerant jet and the gravitational forces.

This process continues over time, causing the development of stratification in the refrigerant concentration as described by (Baines and Turner 1969) and (Nabi and Flynn 2013). Consequently, the simplified well-mixed model will underestimate the refrigerant concentration in some parts of the room and overestimate it elsewhere; however, the current static approach of Standard 15 uses the same assumption, suggesting that this is not necessarily a problem.

One object of the current study is therefore an assessment of the accuracy of these models via a comparison to the more accurate CFD models for a simple scenario of a single room. Since the spatial average of the refrigerant concentration might not be accurately represented by the well-mixed model, information from such a model comparison will be helpful in evaluating the potential application of these models to the problem of predicting refrigerant dispersion dynamics. The refrigerant concentration predicted by the well-mixed models will therefore be compared to the averaged refrigerant concentration, as well as some local concentrations, predicted by the CFD simulations. While these models can be parametrized in a variety of ways, the well-mixed model formulation employed in this paper allows the user to impose both volumetric boundary conditions and pressure-driven boundary conditions. This parametrization is somewhat different than that of (Waye, Petersen and Beyer-Lout 2012), which did not include terms to describe both exhaust ventilation air exchange and air-exchange with an adjacent space, such as a hallway.

This well-mixed model may be formulated by constructing a mass balance equation to solve for the concentration in a room, e.g.,

$$V\frac{dC}{dt} = \dot{m}_{leak} - C(Q_{out} + Q_{exh}) \tag{4}$$

where V is the volume of the room and C is the refrigerant concentration. This model assumes that the exhaust flow rate is constant and is a known value. An analytical solution of the above equation can be found for this problem for a given set of initial conditions; a simple solution for the case in which there is no doorway gap ($Q_{out} = 0$) and the initial concentration $C_{out} = 0$, as well as a constant leakage rate $\dot{m}_{leak}$ and exhaust ventilation rate Q_{exh}, will result in a solution for (4) of

$$C = \exp\left(-\int \frac{Q_{exh}}{V}dt\right)\left[\int \frac{\dot{m}_{leak}}{V}\exp\left(\int \frac{Q_{exh}}{V}dt\right)dt\right] + C_0\exp\left(-\int \frac{Q_{exh}}{V}dt\right) \tag{5}$$

This can be simplified as

$$C = \frac{\dot{m}_{leak}}{V}\left(1 - \exp\left(\frac{Q_{exh}}{V}t\right)\right) \tag{6}$$

which shows that for very large time, and in the absence of a doorway undercut, the concentration may converge to a steady-state value.

One aspect of these models that requires particular attention is the determination of the outlet flow rate Q_{out}. In many common scenarios, there is a forced exhaust ventilation flow rate Q_{exh} but no specified infiltration rate Q_{out}; this quantity will depend on the characteristics of the pressure-driven flow through all of the cracks and gaps in the room. The characterization of such flows can be difficult, and is very sensitive to the choice of parameter values. This difficulty was initially addressed in this work by using the time-varying value of the infiltration rate calculated directly by the CFD simulations in the well-mixed model, rather than including a pressure-driven correlation as well. By using the data from the CFD model, the uncertainty and inaccuracy introduced by the pressure-driven flow model are removed from the system, allowing the essential features of the well-mixed model to be studied and evaluated before introducing the additional complexity of the flow model. Because this well-mixed model is somewhat simpler than a well-mixed model that could be used in practice by an end user, it is referred to as a simple well-mixed model.

Figure 2 illustrates a comparison between the CFD data and the output of the simple well-mixed model for the two leakage rates $\dot{m}_{high}$ and $\dot{m}_{low}$, with a constant exhaust flow rate Q_{exh} set to Q_{high}= 42.47 m^3/h (25 cfm) and door undercut h_o set to h_{low} = 6.35 mm (0.25 in). The upper plot in Figure 2 illustrates averaged and local concentration dynamics for $\dot{m}_{high}$, while the lower plot illustrates the dynamics at the identical locations for $\dot{m}_{low}$; note that the timescales on each plot are different. These local concentration $\bar{C}_{exhaust}$ is measured at the center of the exhaust vent, and the other local concentration $\bar{C}_{undercut}$ is measured at the center of the door undercut.

On the basis of the concentration profiles shown in this figure, it is evident that the simple well-mixed model performs well. The refrigerant concentration field also appears to be reasonably uniform because the local refrigerant concentrations are very close to the average room concentration. The uniformity of the concentration field for the $\dot{m}_{high}$ case is expected, because the high momentum flux from the refrigerant leak is accompanied by a higher rate of entrainment of the ambient refrigerant into the jet, thereby thoroughly mixing the refrigerant and the air together after a brief period of time.

The concentration profiles for the $\dot{m}_{low}$ scenario illustrated in the lower plot also exhibit well-mixed behavior, despite the lower momentum flux of the refrigerant jet. The mixing mechanism in this scenario is made evident by an examination of the air velocity vectors at a plane in the middle of the room at t=3600 s, as illustrated in Figure 3. The inset of this figure, which shows these vectors in the vicinity of the door undercut, shows that large circulation eddies form at the junction of the wall and the floor due to the Q_{high} exhaust flow at the top of the room. These eddies cause the air/refrigerant mixture to bypass the undercut and flow up the wall, so that the concentration $\bar{C}_{undercut}$ is nearly zero. The action of these eddies also serves to mix the room air, causing the local refrigerant concentrations to be very similar to the average concentration. These flow structures are also present in the $\dot{m}_{high}$ scenario, but their effect is less evident because of the mixing that occurs due to the entrainment of the air/refrigerant mixture into the refrigerant jet.

It is also notable that $\bar{C}_{exhaust}$ is initially lower than $\bar{C}_{avg}$ in the $\dot{m}_{low}$ scenario illustrated in Figure 2. Over the first 400 seconds, the well-mixed model does not describe the local behavior at the exhaust fan's location; this is expected because of the long refrigerant transport time. The well-mixed model does appear to represent the average dynamics of the refrigerant concentration reasonably well over longer time periods for this room geometry and set of parameter values.

Figure 4 illustrates some of the effects that are manifest when parameters of the room are changed to examine the sensitivity of these flow dynamics. In this simulation, the exhaust airflow Q_{exh} was reduced to Q_{low}= 42.47 m^3/h (5 cfm) and h_o was increased to h_{high}= 30.48 mm (1.2 in), while the location of the exhaust vent and the refrigerant injection were left the same. Though there are similarities in the concentration dynamics between this scenario and that illustrated in the bottom plot of Figure 2, there are a number of notable differences.

One first observation from this scenario is that there is a significant difference between the local concentrations $\bar{C}_{exhaust}$ and $\bar{C}_{undercut}$ over the duration of the simulation. This suggests that the room stratification is non-negligible, and it is thus not surprising that the simple well-mixed model does not perform as well as before. Examination of the velocity field, illustrated in Figure 5, reinforces the notion that there is less mixing in this scenario; the velocity vectors are much smaller in this case, and there is a measurable current of air/refrigerant mixture leaving of the room through the undercut. Because the eddies created by the exhaust fan have less of an effect on the flow at the floor than was illustrated in Figure 2, there is a greater deviation between the average room concentration and the concentration predicted by the simple well-mixed model. It can still be said that the model describes the overall dynamics of the refrigerant concentration reasonably well, but the sensitivity to parametric variation in Q and h_o is apparent.

Additional parametric variation, through the movement of the location of the injection source, reveals the extent to which the well-mixed model is dependent upon these assumptions. In the simulation illustrated in Figure 6, only the geometric parameters of the refrigerant injection location and the location of the exhaust vent were changed, while the values of the other parameters were maintained at their previous values of $\dot{m}_{ref} = \dot{m}_{low}$, $Q_{exh} = Q_{high}$, and $h_o = h_{low}$. The refrigerant injection location was moved from a point in the middle of ceiling of the room to a point in the middle of the wall in front of the undercut to the hallway, and the exhaust vent was also moved to a location that was 0.5 meters (20 inches) from the floor of the room in the center of the wall adjacent to the undercut.

Despite some of the unusual aspects of the refrigerant concentration field that are illustrated in this figure, it is clear that the well-mixed model does not represent the average room concentration very well. The oscillations in both local concentrations, and particularly in $\bar{C}_{undercut}$, indicate the presence of a ``clogging'' flow dynamic that are caused by the pressure waves and instabilities in the flow, much like what happens when pouring water out of bottle while holding it vertically (Ramamurthi and Nandakumar 1999). While these oscillations may initially be ascribed to numerical instabilities, additional simulations with different temporal and spatial discretizations indicated that these oscillations are based upon physical phenomena. Even after taking these oscillations into consideration, the differences between the local concentrations are large enough to suggest that there is significant stratification in the room. Consequently, these two local concentrations are quite different than both the measured average concentration and the concentration predicted by the simple well-mixed model. It is clear that by only changing geometric aspects of these models, and not taking the geometry of the refrigerant injection location into account, the accuracy of the simple well-mixed model is drastically reduced. Though the simple well-mixed model does perform well in some conditions and is sensitive to the rate of refrigerant leakage, it is quite sensitive to the values of other parameters which affect the level of stratification in the room.

One additional aspect of the simple well-mixed model that must be addressed is the determination of the pressure-driven infiltration or exfiltration volumetric flow rates Q_{out}. Though the CFD simulations have provided sufficient information about the pressure-driven flow rates needed to to study and assess the performance of the simple well-mixed model, this data is usually not available. One method for estimating the pressure-driven flow Q_{out} from readily available parameters uses Dalziel's approach (Dalziel and Lane-Serff 1991),

$$Q_{out} = k(h_{out}W)\sqrt{C\frac{gh_{out}}{\rho_{ref}}} \tag{7}$$

where ρ_{ref} is a reference density. For this equation, the refrigerant concentration is evaluated just inside the connecting space, and is equal to the averaged concentration from the well-mixed model. According to Dalziel's model, the constant $k = 0.21$ for a vertical gap. It is notable that the above equation is similar to the orifice equation, where a value of $C_d = 0.6$ is usually used instead of k. Furthermore, Equation 7 can be substituted into Equation 4 to determine the refrigerant concentration for a given space, e.g.,

$$\frac{dC}{dt} = \frac{\dot{m}_{leak}}{V} - \frac{CQ_{exh}}{V} - Ck\frac{h_{out}W}{V}\sqrt{C\frac{gh_{out}}{\rho_{ref}}} \tag{8}$$

The solution to this equation is more complex in the case of the doorway gap, and a numerical integration routine, such as a Runge-Kutta fourth order scheme, can be used to determine the refrigerant concentration as a function of time for the set of parameters $\dot{m}_{leak}$, Q_{exh}, V, g, h_{out}, and ρ_{ref}.

The performance of this more tractable well-mixed model based on Dalziel's correlation was assessed by comparing it to both the simple well-mixed model results and the average concentration data, which was obtained from the CFD models. The two well-mixed models are illustrated in Figure 7; the upper plot compares these models using the scenario in which the refrigerant injection location was positioned in the middle of the ceiling, originally described in Figure 4, while the lower plot illustrates the comparison between the models using the scenario in which the refrigerant injection location was located on the wall, as described in Figure 6. It is important to again note that the time scales differ between the upper and the lower plots of this figure. It is evident from both of the plots illustrated in Figure 7 that the deviation between the averaged refrigerant concentration obtained from CFD ($\bar{C}_{avg}$) and the prediction from Dalziel's model is larger than the deviation between $\bar{C}_{avg}$ and the prediction from the simple well-mixed model.

In considering this set of results, it is apparent that the dynamic behavior of the flow causes the layers of the air/refrigerant mixture with higher concentration ascent toward the source, and these may even surpass the source concentration in the case of a nonzero momentum flux at the origin (Nabi and Flynn 2014). For some values of exhaust ventilation flow rate, the mixture from the bottom of the room is pulled towards the elevation of the exhaust fan; if the exhaust fan is located close to the floor of the room, the refrigerant concentration will likely be higher at the bottom of the room than it is at the top of the room. When the injection source and the exhaust fan are both at the top of the room, in comparison, it is more likely that the system will exhibit well-mixed behavior. As a result, it might be difficult to justify the use of these models to assess refrigerant safety though all of the models demonstrate generally similar qualitative behavior, as both the size and sign of the error are dependent upon the particular geometric parameters of the room. In the absence of any CFD or experimental data, it therefore seems prudent to recommend only using such models with an abundance of caution. While the sensitivity to the geometric parameters discussed in this work might be approximately predictable, insufficient evidence exists that the prediction errors for the well-mixed models can be reliably bounded, and may yield results that differ from the actual concentration by an order of magnitude or more.

MULTIPLE CONNECTED SPACES

While studies of the dynamics of refrigerant dispersion in single spaces quite useful of themselves, these results can also be used to better understand the dynamics of refrigerant dispersion in multiple connected spaces, which can potentially introduce complex coupling behavior between the single space dynamics. Motivation to study refrigerant dispersion in multiple connected spaces can be found from a variety of applications that benefit from an understanding of how all of the internal spaces of a building are affected by refrigerant leaks, including spaces adjacent to those which contain refrigerant pipes. Particularly common and relevant examples of such scenarios include hotels, commercial office buildings, and multifamily residences. The need to eliminate the ambiguity inherent in the connecting spaces clause of Standard 15 also provides a strong incentive to study this phenomenon.

Due to the potential complexity that can arise in the refrigerant concentration transients for multiple connected spaces, this work is focused on studying the dynamics for two connected rooms, as shown in Figure 1. Many parameters can be used to describe the geometric configuration of the rooms, which we will briefly describe for the sake of clarity. Due to the importance of simulating the behavior of realistic spaces, this work examined a large number of scenarios in which the location and flow rate (Q_{exh}) of the exhaust vent were varied. The size (h_i and w_i) and location of the connecting space between the rooms, like a door undercut or transfer grille, were also varied. In addition, all of the two room simulations included a door undercut between the forced room and an adjacent space, such as a hallway; the dimensions of this undercut were held constant for all of the simulations at 0.914 m (3 ft) wide and 6.35 mm (0.25 in) high.

A number of parameters were varied during these experiments to better understand the dependence of the dispersion dynamics on the particular characteristics of the occupied spaces. The two values for the refrigerant mass flow rate used in the single room experiments, $\dot{m}_{high}$ and $\dot{m}_{low}$, were also used in these experiments. While only one exhaust ventilation rate of Q_{high} was used, the location of the exhaust vent was varied by locating it in either the forced room or the unforced room, and moving it from the ceiling of the unforced room to a position low on the wall of the unforced room. The height h_i and width w_i of the connecting space were also varied over a range of values to explore the effect on the dispersion dynamics. While the height and depth of the unforced room were held constant, the width of the room perpendicular to the wall adjoining the two rooms was also varied.

In the first set of simulations, the effect of varying the refrigerant mass flow rate into the forced room when the exhaust vent is located in the unforced room and the parameters of the door undercut are h_i= 6.35 mm (0.25 in) and w_i= 0.90 m (3 ft) were studied, as shown in Figure 8. The upper plot illustrates the concentration profiles in both the forced and the unforced rooms over a period of 1800 seconds due to a leakage rate of $\dot{m}_{high}$, while the lower plot illustrates the concentration transient over 7200 seconds for the $\dot{m}_{low}$ leakage rate. By comparing the temporal evolution of the concentrations in both rooms, it is clear that the refrigerant is distributed in both rooms for both leakage rates even for the small connecting space with an opening area of 9 in^2. Moreover, the refrigerant concentration profile in both rooms is quite similar in the $\dot{m}_{low}$ scenario illustrated in the lower plot, indicating that the refrigerant is distributed between both rooms, and that the effects of the low leakage rate and the exhaust vent combine to prevent the refrigerant concentration from reaching the RCL.

The differences in the refrigerant concentration profiles between forced room and the unforced room in the $\dot{m}_{high}$ experiment are particularly notable. In this scenario, the transport time of the refrigerant from the forced room to the unforced room is much greater than the duration of time over which the refrigerant enters the room. The maximum refrigerant concentration in the forced room thus occurs before a significant mass of refrigerant has entered the unforced room. Over time, however, the refrigerant in the forced room is gradually convected into the unforced room, causing the refrigerant to gradually redistribute. In comparing the $\dot{m}_{high}$ scenario to the $\dot{m}_{low}$ scenario for these model assumptions, it appears that the dispersion dynamics in both of the connected rooms are quite dependent upon the leakage rate; a high rate leak results in a higher initial concentration in the forced room with the other room concentration lagging, while a low-rate leak distributes the refrigerant through both rooms more uniformly.

The dependence of the refrigerant distribution on the size of the connecting space is studied in the next set of simulations. The exhaust vent was located in the unforced room and the refrigerant leakage rate $\dot{m}_{low}$ was used in all of these scenarios. A variety of sizes for the door undercut were used in these simulations; three simulations used an undercut with height h_i= 6.35 mm (0.25 in) and a width w_i equal to 3.05 m (10 ft), 0.91 m (3 ft), and 0.15 m (6 in), which are called ``full width (fw)'', ``partial width (pw)'', and ``tiny width (tw)'' respectively. The fourth simulation, denoted ``large (lg),'' used a much larger connecting space with h_i= 0.76 m (30 in) and w_i= 1.52 m (60 in) for comparison with the other smaller undercuts. The results of these simulations can be seen in Figures 9 and 10; the concentration profiles for the forced room are illustrated in Figure 9, while the concentration profiles for the unforced room can be seen in Figure 10.

One particularly interesting result that is evident from these simulations is that the size of the connecting space has a negligible effect on the distribution of refrigerant between both of the rooms. This can be clearly seen because the refrigerant distribution for the scenario with the tiny width undercut is nearly identical to the refrigerant distribution with the full width undercut. The lower plots in both of these figures illustrate the difference between the partial width and full width undercuts, as well as the tiny width and full width undercuts; the magnitude of these differences are on the order of 1% of the total refrigerant concentration. While this may initially appear to be counterintuitive, further reflection reveals that fixing the volumetric flow rate of air out of the exhaust vent, located in the unforced room, will constrain the total flow rate from the forced room into the forced room. Changes in the surface area of the connecting space will therefore result in corresponding changes in the velocity of the air passing through the undercut in inverse proportion to the changes in the surface area, but will not change the rate of air exchange between both rooms.

Support for this logic is further strengthened by consideration of the ``large" connecting space. Simulations for the dynamic behavior of the refrigerant concentration in both rooms with this connecting space, which has an area 60 times larger than that of the ``full width" connecting space, indicate that though the refrigerant concentrations differ by approximately 10% after 3600 seconds, the overall behavior of the refrigerant concentration is very similar. In consideration of these results, this variety of simulations suggests that all connecting spaces are essentially equivalent under the influence of forced ventilation, and that the size of the connecting space does not affect the dynamics of the refrigerant distribution between all of the multiple spaces.

Simulations were also run to study the effect of changing various geometric parameters for the unforced room on the overall concentration dynamics. During these tests, the refrigerant dispersion rate was maintained at $\dot{m}_{low}$ and the ``partial width" connecting space was used, while the location of the exhaust vent in the unforced room was moved from the initial location in the corner of the ceiling opposite the wall which housed the undercut to a position in the middle of the wall opposite the undercut, and the width of the unforced room was also doubled. The results from these simulations are shown in Figure 11, where the concentration profiles for the forced room are shown in the upper plot and the concentration profiles for the unforced room are shown in the lower plot. In this figure, the baseline data with the exhaust vent located on the ceiling and the original room width is labeled $\bar{C}_{ceiling}$, while the data with the changed exhaust vent location is labeled $\bar{C}_{wall}$ and the data with the changed room width is labeled $\bar{C}_{equal}$.

It is clear from the concentration profiles seen in the upper plot of Figure 11 that the concentration in the forced room does not depend on changes in the geometric parameters of the unforced room. This is expected because the boundary conditions for the forced room do not depend on the geometric configuration of the unforced room. In comparison, the concentration profiles for the unforced room do depend strongly on the geometric parameters. These results are consistent with those reported earlier in (Laughman, Nabi and Grover 2015). By moving the exhaust vent location from the ceiling to the middle of the wall, the exhaust vent removes air with a higher local concentration of refrigerant, causing the average refrigerant concentration in the unforced room to increase more slowly. Doubling the width of the unforced room also effectively reduces the average concentration, as would be expected because the average is taken over a much greater volume. However, the concentration profiles for both room sizes converge near 3600 seconds, which is expected as the refrigerant continues to mix in the unforced room.

In the final set of simulations of the two rooms, the exhaust vent was moved from the unforced room to the forced room and the dimensions of the connecting space were also varied. Both the partial width and large connecting spaces, as seen in Figures 9 and 10, were used in the simulation where the exhaust vent was located in the forced room, while only the partial width connecting space was used in the simulation with the exhaust vent located in the unforced room. For all of these simulations, the location of the exhaust vent remained on the ceiling and the refrigerant flow rate used was $\dot{m}_{low}$. These results can be seen in Figure 12; as before, the concentration profiles for the forced room are illustrated in the upper plot, while the concentration profiles for the unforced room are illustrated in the lower plot.

The plots in this figure demonstrate the significant differences in the dispersion dynamics that result when the location of the exhaust vent is moved between rooms. While the simulation in which the exhaust vent is located in the unforced room shows that refrigerant is distributed between both rooms, the simulation in which the exhaust vent is located in the forced room with a partial undercut shows that very little refrigerant enters the unforced room. This clearly results in a much lower refrigerant concentration in the unforced room, and also in a marginally higher concentration for the forced room because of the higher refrigerant concentration of the exhausted air. In comparison, more refrigerant does enter the unforced room in the scenario with the large connecting space, but the concentration profile in the unforced room in this scenario is still lower than it is in the scenario with the exhaust in the unforced room.

These results emphasize the important role that the location of the exhaust vent plays in the multiple connected spaces problem; if the forced air is located in the space without the leak, the refrigerant will clearly be convected with the pressure-driven flow. In addition, the comparison between the partial width and large connecting space profiles indicate that the size of the connecting space does play an important role in distributing refrigerant when the exhaust vent is in the forced room, but that the size of the connecting space is less important when the exhaust vent is in the unforced room.

In general, these simulations highlight the important effect that ventilation has on multiple connected spaces, as the location and direction of airflow has a significant impact on the dynamics of the refrigerant dispersion. Scenarios in which the exhaust vent was located in the unforced space all resulted in the distribution of refrigerant throughout both spaces, while scenarios in which the exhaust vent was located in the forced room resulted in a much lower rate of refrigerant distribution into the unforced space. Where the exhaust vent is located in a space adjacent to that of the refrigerant leak, the size of the connecting space did not have a significant influence on the rate of refrigerant dispersion, and even small connecting spaces were sufficient to allow the refrigerant to be distributed throughout both spaces. These simulations also emphasized the fact that the timescales of refrigerant distribution are strongly dependent upon the refrigerant leakage rate, and that the dynamics of the forced room do not depend on the geometry of the unforced room.

CONCLUSIONS AND FUTURE WORK

With the increasing global demand for comfort conditioning and the attendant development of an ever-evolving range of applications for vapor-compression cycles, knowledge about the dynamics of refrigerant dispersion in occupied spaces will continue to be a salient concern for a wide array of segments of the building industry. In addition, increased understanding must be accompanied by a range of models and tools that enable the application of this knowledge to practical situations involving the design, commissioning, and operation of these systems in the field. The work described in this paper addresses both of these needs: the dynamics of refrigerant dispersion in multiple connected spaces were explored parametrically, and the accuracy of low-complexity models that are amenable to application in routine situations was assessed. In general, the well-mixed models are sensitive to the changes in the leakage rate, but not to changes in geometric parameters; as a result, such models should be used with caution and with their limitations in mind. The two-room studies characterized the dependence of the concentration profiles in both rooms on the size of the connecting space, the leakage rate, and the location of the exhaust vent.

The resulting CFD data indicated that the location of the exhaust vent has a significant influence on the dispersion dynamics, and that the size of the connecting volume has a much smaller effect.

Though this paper constitutes an extensive investigation of both low-order modeling approaches and the dispersion dynamics in multiple connected spaces, the work has only scratched the surface of a wide variety of problems related to this area. For example, the reports obtained from KHK may be used as a foundation for a quantative analysis of the rate of faults, and the combination of such data with the modeling approaches found in this paper may enable new fault tree analyses that provide quantitative risk assessment tools for buildings. New and improved low-complexity models for the dispersion dynamics for both single and multiple connected spaces, as well as frameworks for adjusting the complexity of these models dynamically, would also be quite useful. Finally, physical experiments that validated the simulations and analysis performed in this work would serve to both validate current understanding and point in the direction of greater improvement and general benefit.

ACKNOWLEDGEMENTS

The authors would like to thank Mitsubishi Electric Cooling & Heating, a division of Mitsubishi Electric US, Inc., for their generous support of this work. We also would extend our thanks to Osami Kataoka and Kenji Inomata for their contributions to our understanding of the statistics from KHK. Dan Burns and other reviwers also provided valuable feedback that improved this paper.

REFERENCES

"ANSYS CFX-Pre User's Guide, Release 15.0." 2014.

ASHRAE Standard 15. "Safety Standard for Refrigation Systems." Standard, American Society of Heating, Refrigeration, and Air Conditioning Engineers, Inc., Atlanta, GA, 2010.

ASHRAE Standard 34. "Designation and Safety Classification of Refrigerants." Standard, American Society of Heating, Refrigeration, and Air-Conditioning Engineers, Inc., Atlanta, GA, 2010.

ASHRAE Standard 62.1. "Ventilation for Acceptable Indoor Air Quality." Standard, American Society of Heating, Refrigeration, and Air Conditioning Engineers, Inc., Atlanta, GA, 2013.

Baines, W.D., and J.S. Turner. "Turbulent buoyant convection from a source in a confined region." *Journal of Fluid Mechanics* 37 (1969): 51-80.

Bird, R.B., W.E. Steward, and E.N. Lightfoot. *Transport Phenomena.* 2. John Wiley and Sons, Inc., 2006.

Dalziel, S.B., and G.F. Lane-Serff. "The hydraulics of doorway exchange." *Building and Environment* 26, no. 2 (1991): 121-135.

Duda, Stephen W. "Applying VRF? Don't overlook Standard 15." *ASHRAE Journal* 54 (July 2012): 18-24.

Hihara, E. "Risk Assessment of Mildly Flammable Refrigerants: 2013 Progress Report." Tech. rep., The Japan Society of Refrigerating and Air Conditioning Engineers, 2014.

ISO 5149-3. "Refrigerating Systems and Heat Pumps - Safety and Environmental Requirements." Standard, International Organization for Standardization, Geneva, Switzerland, 2014.

Kataoka, O. "Personal correspondence." unpublished, 2015.
Kataoka, O., S. Ishida, T. Hirakawa, and M. Yoshizawa. "Experimental and numerical analyses of refrigerant leaks in a closed room." *ASHRAE Transactions* 105 (1999): 1-8.
Kataoka, Osami. (April 2015).
KHK. *Refrigation and Air-Conditioning News.* Vol. 38. Kouatsu-Gas Hoan Kyoukai (KHK), 2014.
Laughman, C.R., S. Nabi, and P. Grover. "A study of refrigerant dispersion in occupied spaces under parametric variation." *ASHRAE Annual Meeting.* 2015.
Lewandowski, T., and K.R. Reid. "Risk assessment for residential heat pump systems using 2{L} flammable refrigerants." *ASHRAE/NIST Refrigerants Conference.* 2012.
Nabi, S., and M.R. Flynn. "Influence of geometric parameters on the eventual buoyancy stratification that develops due to architectural exchange flow." *Building and Environment* 71, no. 1 (2014): 33-46.
Nabi, S., and M.R. Flynn. "The hydraulics of exchange flow between adjacent confined building zones." *Building and Environment* 59, no. 1 (2013): 76-90.
Nagaosa, R., V. Aute, and R. Radermacher. "A risk assessment for leakages of flammable refrigerants into a closed space." *International Refrigeration and Air Conditioning Conference at Purdue.* 2012.
Okamoto, H., T. Hattori, C. Dang, and E. Hihara. "Simulation of mildly flammable refrigerants." *15th International Refrigeration and Air Conditioning Conference at Purdue.* 2014.
Ramamurthi, K., and K. Nandakumar. "Characteristics of flow through small sharp-edged cylindrical orifices." *Flow Measurement and Instrumentation* 10 (1999): 133-143.
Reindl, D.T. "Celebrating 100 years of ASHRAE Standard 15." *ASHRAE Journal* 56 (November 2014): 36-43.
UL 484. "Room Air Conditioners." Standard, Underwriters Laboratories, 2012.
Waye, S.K., R.L. Petersen, and A. Beyer-Lout. "Ventilation requirements for refrigerating machinery rooms." *ASHRAE Transactions* 118 (2012): 491-507.
White, Frank. *Viscous Fluid Flow.* 2. McGraw-Hill, 2005.

FIGURES

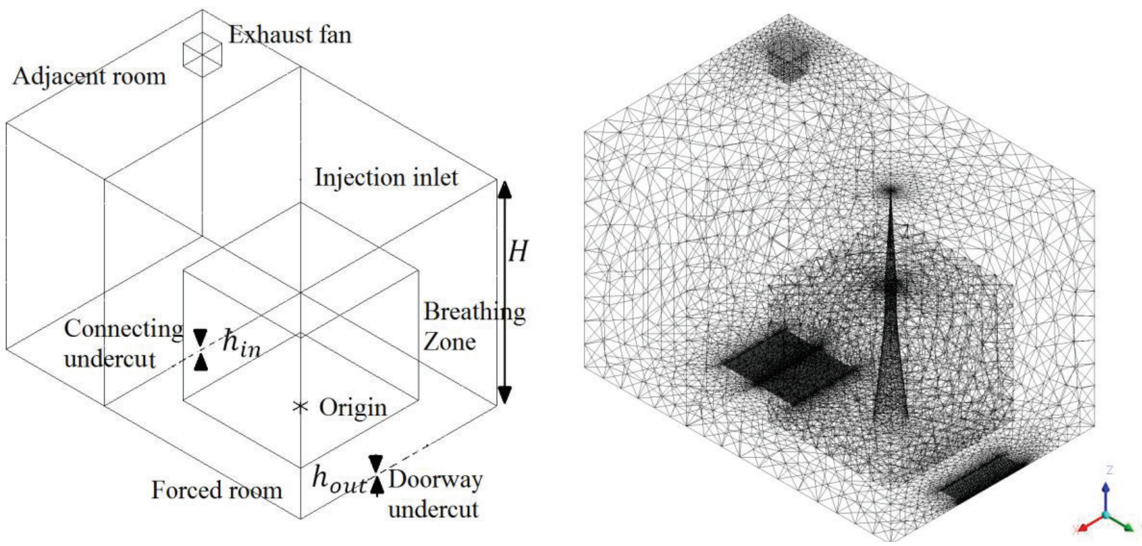

Figure 1: Schematic drawings for single and multiple room simulations.

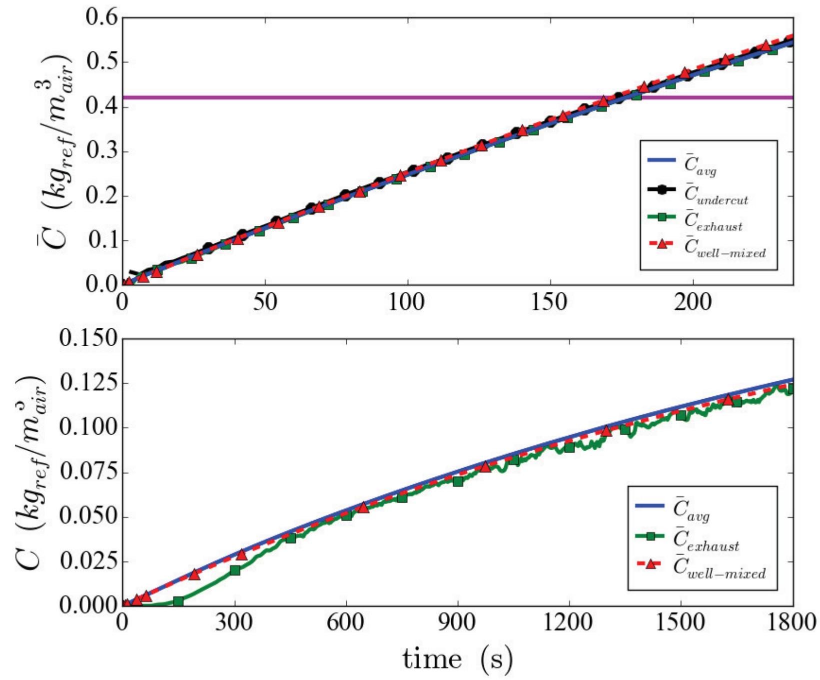

Figure 2: Average and local refrigerant concentrations in single room, as well as output of simple well-mixed model, for $\dot{m}_{high}$ and $\dot{m}_{low}$ with constant Q_{high} and $h_{o,low}$.

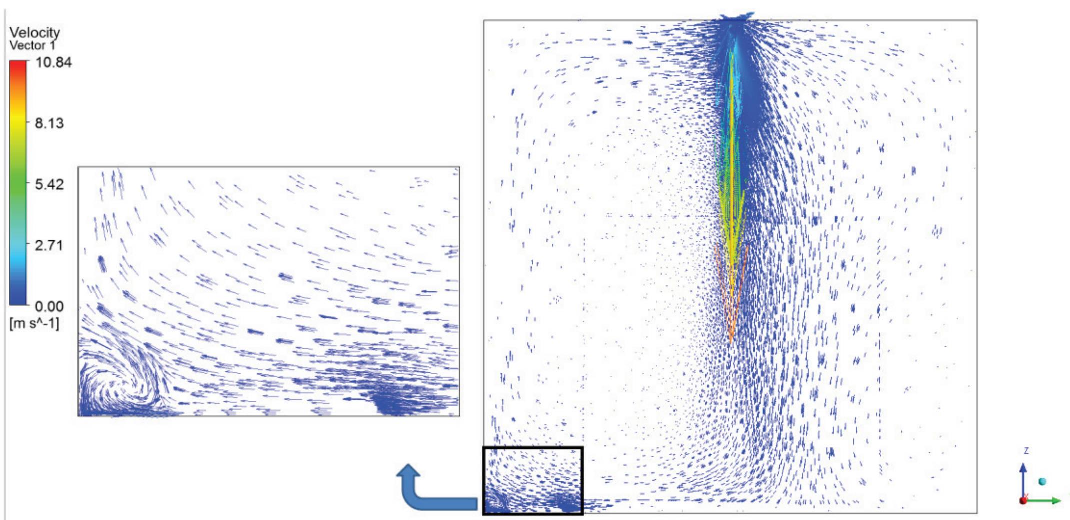

Figure 3: Velocity field in room for the parameter set ($\dot{m}_{low}$, Q_{high}, $h_{o,low}$), illustrating the reach of the fan and its effect in mixing the air in the room.

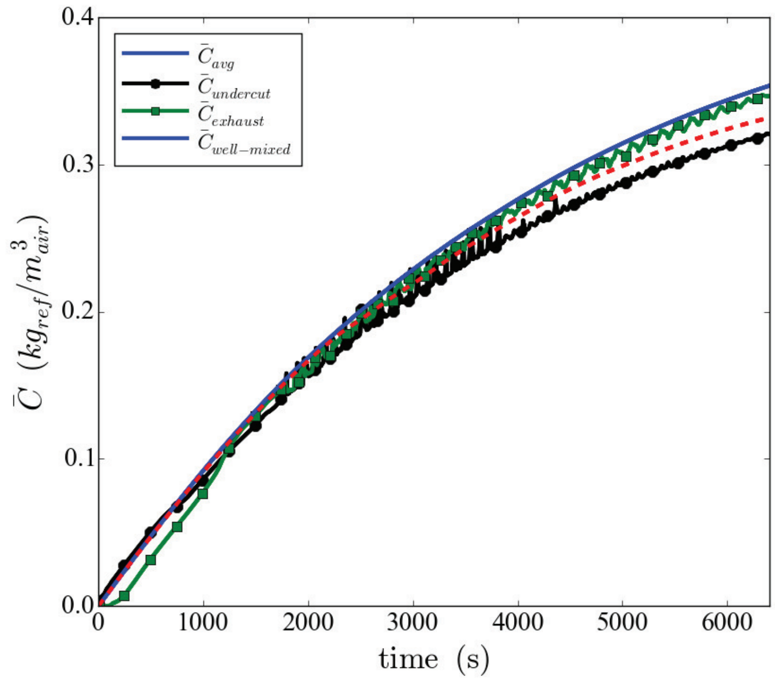

Figure 4: Average and local refrigerant concentrations in single room, as well as output of simple well-mixed model, for the parameter set ($\dot{m}_{low}$, Q_{high}, $h_{o,low}$).

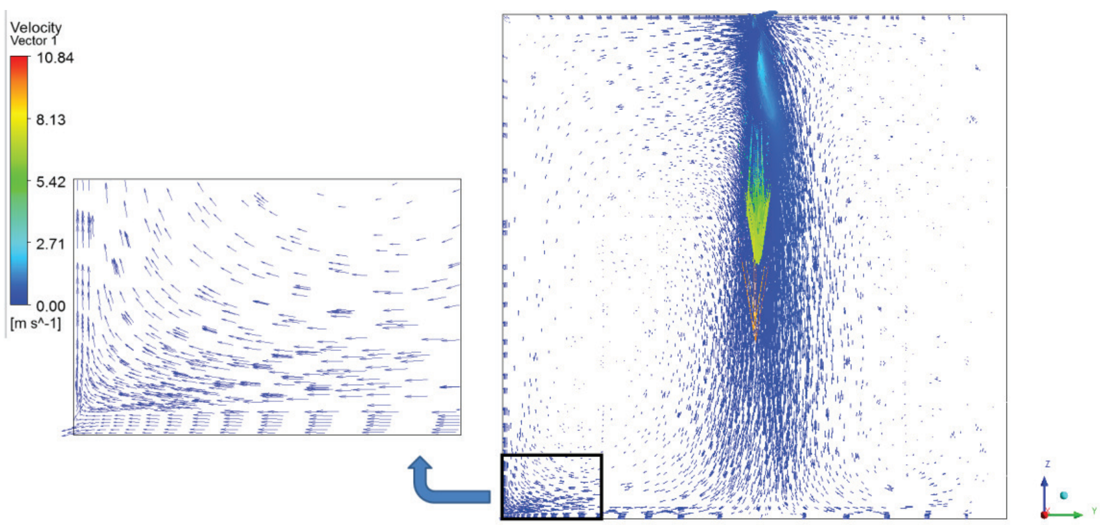

Figure 5: Velocity field in room for the parameter set ($\dot{m}_{low}$, Q_{low}, $h_{o,high}$), illustrating the reach of the fan and its effect in mixing the air in the room.

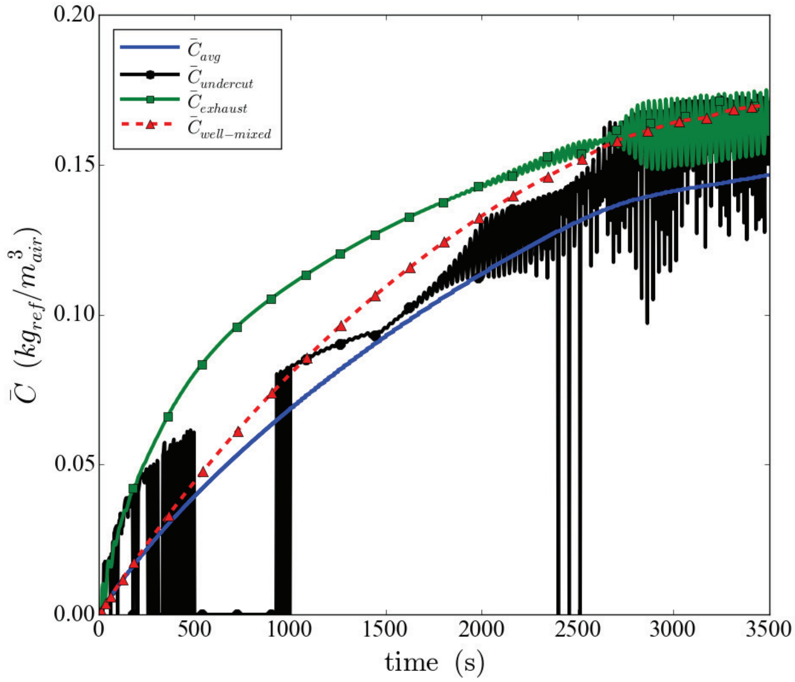

Figure 6: Average and local refrigerant concentrations in single room, as well as output of simple well-mixed model, for the parameter set ($\dot{m}_{low}$, Q_{high}, $h_{o,low}$) when the injection source is located on the wall of the room and the exhaust vent is located 0.5 meters above the floor.

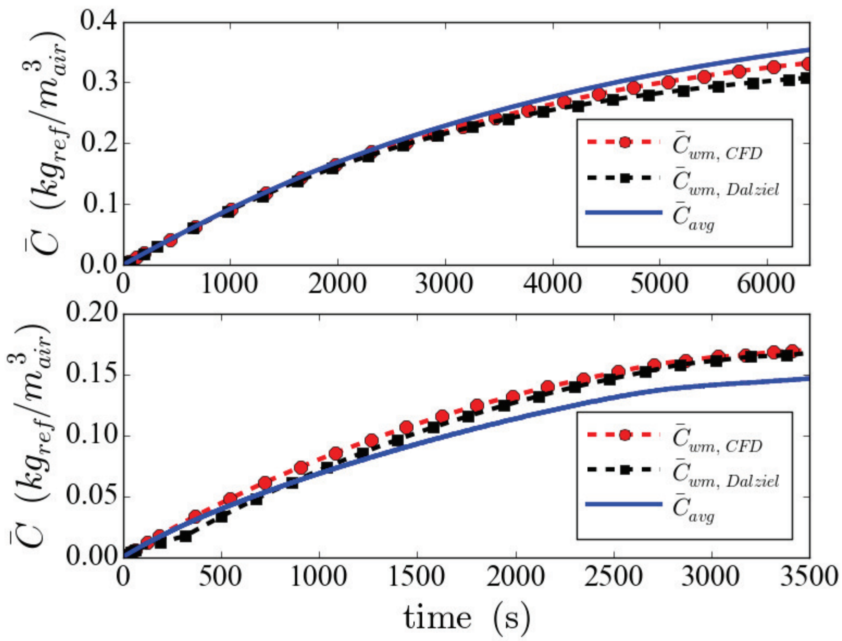

Figure 7: Average and local refrigerant concentrations in single room, as well as output of simple and

Dalziel well-mixed models, for different scenarios.

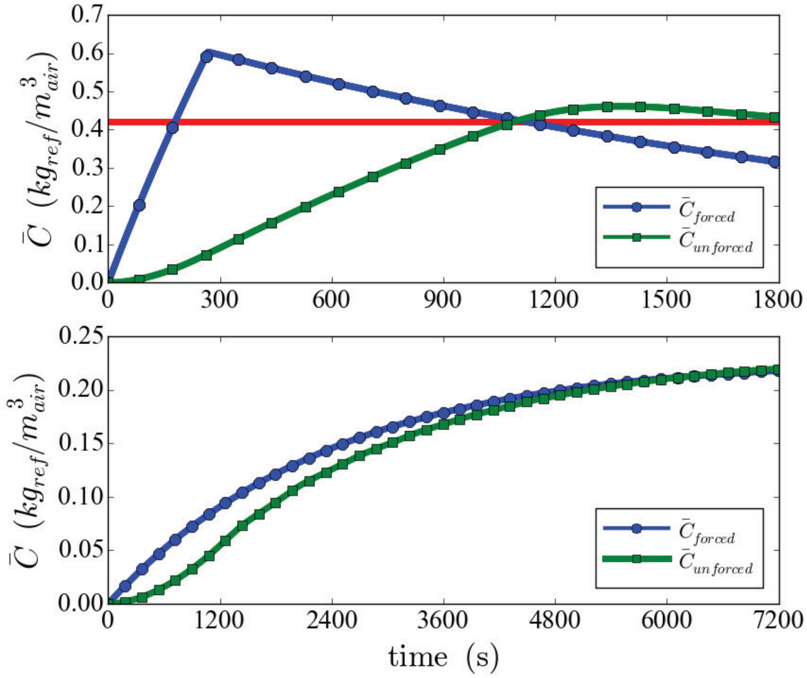

Figure 8: Average and local refrigerant concentrations in connected rooms, as well as output of simple well-mixed model, for $\dot{m}_{high}$ and $\dot{m}_{low}$ with constant Q_{high} and h_i..

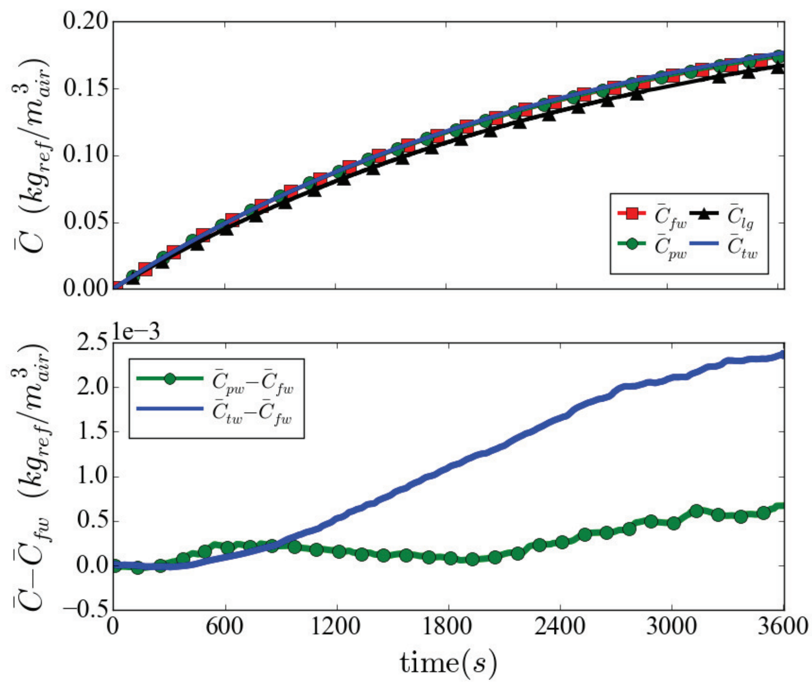

Figure 9: Average refrigerant concentrations and residuals for the forced room for $\dot{m}_{low}$, h_i = 0.25in, and w_i = (10ft, 3ft and 0.5ft).

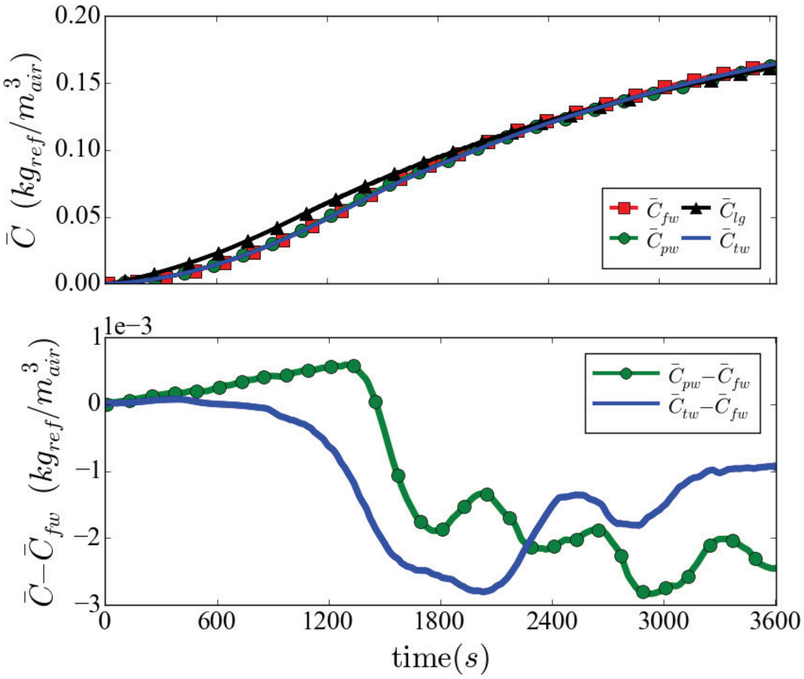

Figure 10: Average refrigerant concentrations and residuals for the unforced room for $\dot{m}_{low}$, h_i = 0.25in, and w_i = (10ft, 3ft and 0.5ft).

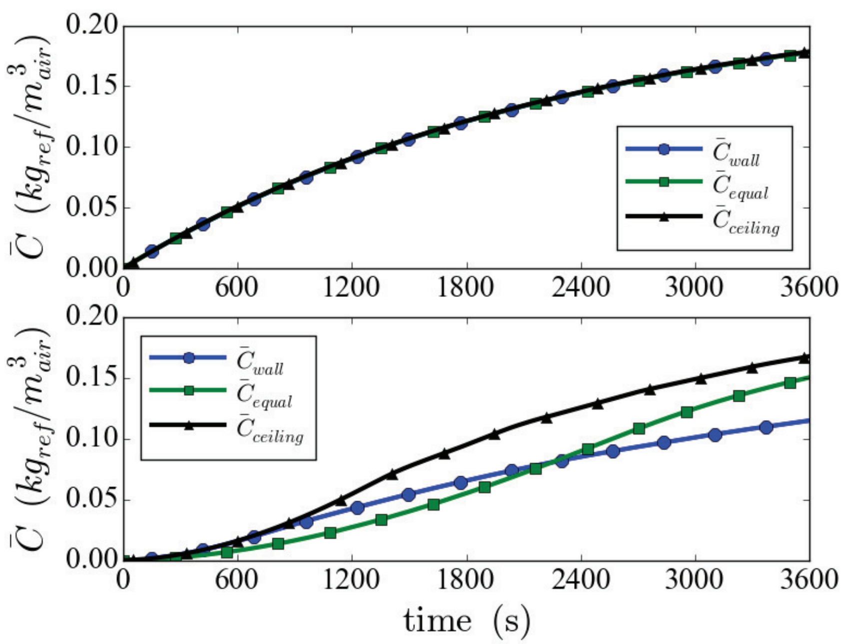

Figure 11: Average refrigerant concentrations and residuals for the forced and unforced rooms when varying the refrigerant injection location and the width of the unforced room, for $\dot{m}_{low}$, h_i = 0.25in, and w_i = (10ft, 3ft and 0.5ft).

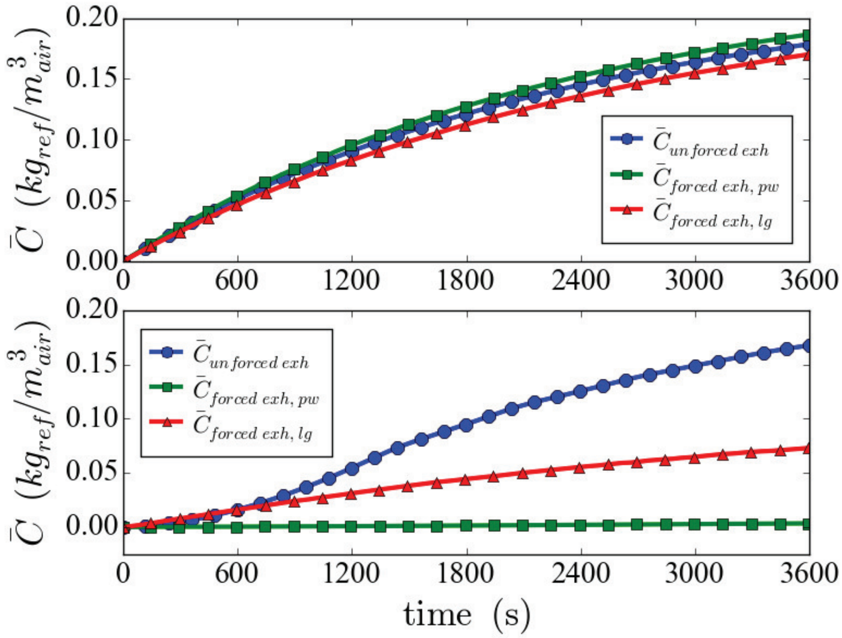

Figure 12: Average refrigerant concentrations and residuals for the forced and unforced rooms when varying the location of the exhaust vent between the different rooms, with $\dot{m}_{low}$, h_i = 0.25in, and w_i = 3ft.